jove

Co-culture of Glutamatergic Neurons and Pediatric High-Grade Glioma Cells Into Microfluidic Devices to Assess Electrical Interactions

Quentin Fuchs[1], **Aurélie Batut**[2], **Mélanie Gleyzes**[2], **Jessica Rontard**[2], **Louise Miny**[2], **Margot Libralato**[2], **Janaina Vieira**[2], **Delphine Debis**[2], **Florian Larramendy**[2], **Thibault Honegger**[2], **Melissa Messe**[1], **Marina Pierrevelcin**[1], **Benoit Lhermitte**[1,3], **Monique Dontenwill**[1], **Natacha Entz-Werlé**[1,4]

[1] Team Tumoral signaling and therapeutic targets, UMR CNRS 7021 - Laboratory of Bioimaging and Pathologies [2] NETRI [3] Centre de Ressources Biologiques, Pathology department, University Hospital of Strasbourg [4] Pediatric Oncohematology unit, University Hospital of Strasbourg

Corresponding Author

Natacha Entz-Werlé

Natacha.entz-werle@chru-strasbourg.fr

Citation

Fuchs, Q., Batut, A., Gleyzes, M., Rontard, J., Miny, L., Libralato, M., Vieira, J., Debis, D., Larramendy, F., Honegger, T., Messe, M., Pierrevelcin, M., Lhermitte, B., Dontenwill, M., Entz-Werlé, N. Co-culture of Glutamatergic Neurons and Pediatric High-Grade Glioma Cells Into Microfluidic Devices to Assess Electrical Interactions. *J. Vis. Exp.* (177), e62748, doi:10.3791/62748 (2021).

Date Published

November 17, 2021

DOI

10.3791/62748

URL

jove.com/video/62748

Abstract

Pediatric high-grade gliomas (pHGG) represent childhood and adolescent brain cancers that carry a rapid dismal prognosis. Since there is a need to overcome the resistance to current treatments and find a new way of cure, modeling the disease as close as possible in an *in vitro* setting to test new drugs and therapeutic procedures is highly demanding. Studying their fundamental pathobiological processes, including glutamatergic neuron hyperexcitability, will be a real advance in understanding interactions between the environmental brain and pHGG cells. Therefore, to recreate neurons/pHGG cell interactions, this work shows the development of a functional *in vitro* model co-culturing human-induced Pluripotent Stem (hiPS)-derived cortical glutamatergic neurons pHGG cells into compartmentalized microfluidic devices and a process to record their electrophysiological modifications. The first step was to differentiate and characterize human glutamatergic neurons. Secondly, the cells were cultured in microfluidic devices with pHGG derived cell lines. Brain microenvironment and neuronal activity were then included in this model to analyze the electrical impact of pHGG cells on these micro-environmental neurons. Electrophysiological recordings are coupled using multielectrode arrays (MEA) to these microfluidic devices to mimic physiological conditions and to record the electrical activity of the entire neural network. A significant increase in neuron excitability was underlined in the presence of tumor cells.

Introduction

Pediatric high-grade gliomas (pHGG) exhibit an extended genotypic and phenotypic diversity depending on patient age, tumor anatomical location and extension, and molecular drivers[1]. They are aggressive brain tumors that are poorly

controlled with the currently available treatment options and are the leading cause of death related to brain cancers in children and adolescents[2]. So, more than 80% of patients are relapsing within 2 years after their diagnosis, and their median survival is 9-15 months, depending on brain locations and driver mutations. The absence of curative treatment is the primary urge for laboratory research and highlights the immediate need for new innovative therapeutic approaches. For this purpose, patient-derived cell lines (PDCL) were developed with the hope of providing the pHGG diversity[3] in two-dimensional (2D) lines and/or three-dimensional (3D) neurospheres. Nevertheless, those patient-derived *in vitro* cell cultures do not mimic all brain variable situations. These models do not consider the macroscopic and microscopic neuro-anatomical environments typically described in pHGG.

Usually, pHGG in younger children is mainly developing in pontine and thalamic regions, whereas adolescent and young adult's HGG concentrate in the cortical areas, especially in frontotemporal lobes[1]. These location-specificities across pediatric ages seem to involve different environments leading to gliomagenesis and an intricating network between tumor cells and specific neuronal activity[4,5,6]. Although mechanisms are still not identified, pHGG mainly develops from neural precursor cells along the differentiation trajectory of astroglial and oligodendroglial lineages. While the role of these glial lineages has been for long restricted to simple structural support for neurons, it is now clearly established that they integrate entirely into neural circuits and exhibit complex bi-directional glial-neuronal interactions able to reorganize structural regions of the brain and remodel neuronal circuitry[4,7,8]. Moreover, increasing shreds of evidence indicate that the central nervous system (CNS) plays a critical role in brain cancer initiation and progression. Recent works focused on neuronal activity, which seems to drive growth and mitosis of glial malignancies through secreted growth factors and direct electrochemical synaptic communications[6,9]. Reciprocally, high-grade glioma cells seem to influence neuronal function with an increasing glutamatergic neuronal activity and modulate the operation of the circuits into which they are structurally and electrically integrated[9]. So, studies using patient-derived models and novel neuroscience tools controlling neuron action demonstrated a circuit-specific effect of neuronal activity on glioma location, growth, and progression. Most of these neuronal projections involved in gliomas are glutamatergic and communicate through glutamate secretions. Specific glutamatergic biomarkers such as mGluR2 or vGlut1/2 are commonly described[6].

Interestingly, despite their molecular heterogeneity, pediatric and adult high-grade gliomas show a typical proliferative response to glutamatergic neuronal activity and other secreted factors such as neuroligin-3 or BDNF (brain-derived neurotrophic factor)[4,6,10,11,12,13]. In cortical regions, pediatric and adult HGGs can induce neuronal hyperexcitability through an increased glutamate secretion and inhibit GABA interneurons leading to gliomas associated with epileptic network activity[14,15]. On top of that, neural circuits can be remodeled by gliomas pushing specific neurological tasks, for instance, language, and can requisition additional organized neuronal activity[9].

Based on this rationale, advancing the understanding of bidirectional communications between glioma cells and neurons must be fully elucidated and integrated with the early stages of *in vitro* pHGG approaches. Such innovative modeling is crucial in understanding and measuring the neuronal electrical activity impact during drug testing and anticipating pHGG response

into brain circuitry. Recent developments in neuroscience tools, such as microfluidic devices and pHGG research works, are the bed to develop new modeling approaches and be able now to integrate brain microenvironment in *in vitro* pHGG models[3,16,17,18,19]. Coupled with electrophysiological recordings using multielectrode arrays (MEA), microfluidic devices[20,21,22] offer the possibility to mimic physiological conditions while recording the electrical activity of the entire neural network and extract network connectivity parameters under several conditions. This device[23,24] allows first the precise deposition of cells in a chamber directly on MEA. This technology enables the control of cell seeding density and homogeneity on MEA and the fine control of media exchange, which is a critical step for human neural progenitor differentiation directly into devices. Moreover, the present deposition chamber can be seeded with multiple cells at different time points.

So, this study aimed to develop a functional *in vitro* model co-culturing human Pluripotent Stem (hiPS)-derived cortical glutamatergic neurons and pHGG-derived cells into microfluidic devices and recording their electrical activity to evaluate electrical interactions between both cell populations. First, hiPS-derived cortical glutamatergic neurons were obtained and characterized in microfluidic devices at different stages of culture [day 4 (D4), as hiPS cells, and day 21 (D21) and day 23 (D23), as glutamatergic matured neurons]. For the second step of co-culture, two pHGG models were used: commercialized pediatric UW479 line and pHGG cells initiated from a patient tumor (BT35)[3], bearing an H3.3 K27M driver mutation. Finally, we performed electrophysiological recordings of glutamatergic cells at D21 before pHGG cell seeding and D23 after 48 h of co-culture into the same microfluidic device. The interactions between glutamatergic neurons and pHGG cells were characterized by a significant increase in the recorded electrophysiological activity.

Protocol

For this protocol, the accreditation number related to the use of human materials is DC-2020-4203.

1. Microfluidic device fabrication, preparation and treatment

1. Fabricate SU-8 molds using conventional photolithography techniques[18].
   NOTE: For this purpose, two photolithography masks have been designed to construct two layers of photoresist structures on silicon wafer substrate and a thin SU-8 2005 photoresist layer (3.2 µm high and 6 ± 1 µm wide) that defines asymmetric microgrooves under the patterning of main channels made in SU-8 2100 (200 µm high, 1 mm wide, and 13 mm long) (see **Supplemental Figure S1**).
2. Activate the wafer by using a plasma cleaner ($5.00e^{-1}$ torr, high radio frequency (RF) level) for 1 min and silanize it using 1 mL of (trichloro(1H,1H,2H,2H-perfluorooctyl)silane in an aluminum folder into a desiccator for 30 min.
3. Prepare a 10:1 ratio of Polydimethylsiloxane (PDMS), mix the prepolymer with catalyst, pass it in a vacuum desiccator to remove trapped bubbles, and cast it slowly onto the mold before being cured in an oven at 80 °C for 40 min.
4. Cut it after that using a razor at the desired size before peeling off the mold. Punch out the inlet and the outlet zones to obtain 3 mm wide holes, clean the PDMS, and protect it using adhesive tape.

NOTE: The thickness of the final PDMS device is approximately 5 mm.

5. Treat the device using a plasma cleaner ($5.00e^{-1}$ torr, High RF level during 1 min), assemble it with a polystyrene Petri dish, and expose the vacuum under UV light for 30 min.

6. Fill with a pipette the inlet of the microfluidic device before usage with 70% ethanol and empty it by pipetting aspiration.

7. Wash the microfluidic device by adding inlet reservoirs Dulbecco's Phosphate Buffered Saline (D-PBS) and empty it by pipetting aspiration three consecutive times.

8. Coat the device using 0.05 mg/mL Poly-D-Lysine and place it into an incubator (37 °C, 5% CO_2). After 24 h, rinse the device by adding into the inlet reservoir the neurobasal medium and empty it by pipetting aspiration three consecutive times.

9. Fill the microfluidic chip with the cell culture medium and let it remain at room temperature until use for a maximum of 2 h.

2. Cell preparation and seeding in the microfluidic device

1. **Culture, seeding, and immunofluorescent characterization of human hiPS-derived cortical glutamatergic neurons**

   NOTE: Carry out experiments with commercialized hiPS-derived cortical glutamatergic neurons (**Figure 1A**). Preserve human-derived materials and handle them with the approval and under the guidelines of legislation.

   1. Empty the inlet and outlet reservoirs of the microfluidic device by pipette aspiration before seeding, letting only the device's channels to be filled with medium.

   2. Seed the hiPS cells at Day 0 (D0) by putting 10 µL of a 6.5 x 10^6 hiPS cells/mL suspension (e.g., 900 cell/mm^2 concentration) with the medium, whose composition is given in **Table 1**, and let the device be under the hood (at room temperature) for 15 min to allow cells to attach.

   3. After 15 min, fill both inlet and outlet reservoirs with 50 µL of D4 culture medium, whose entire composition is given in **Table 1**, and transfer the device into the incubator (37 °C, 5% CO_2).

   4. Maintain glutamatergic neuron differentiation for 23 days (**Figure 1A(1)**, microscopy) under a controlled environment (37 °C, 5% CO_2) and with a specific cell culture medium, whose composition is described in **Table 1**. Replace the medium regularly as detailed in the next step 5. just below and follow the steps as in **Figure 1B**.

   5. Replace the medium every 3 to 4 days following **Table 1** composition. Use seeding medium until D4, D4 medium until D7, D7 medium until D11, and D11 medium for the remaining time of the culture.

   6. Take microscopic pictures at D4, D21, and D23 using a standard phase-contrast microscope to assess cell viability and allow cell counting.

   7. For characterization, fix the differentiated glutamatergic neurons in 4% paraformaldehyde (PFA) for 30 min at room temperature after medium aspiration and follow the protocol for immunofluorescence staining.

8. Wash cells three times with Phosphate-Buffered Saline (PBS) and permeabilize them for 10 min with 0.1% Triton-X followed by 30 min with 3% Bovine Serum Albumin (BSA). Add primary antibodies and incubate the device overnight at 4 °C.

9. Rinse the cells three times with PBS and incubate further with the corresponding secondary antibodies for 2 h at room temperature.
   NOTE: Immunofluorescent antibodies used in the study are listed in **Table 2**.

10. Rinse the cells three times with PBS and counterstain with DAPI (4',6-diamino-2-phenylindole) for 10 min at room temperature.

11. Acquire images with an inverted epifluorescence microscope fitted with a CMOS (Complementary metal-oxide-semiconductor) camera and analyze using appropriate image analysis software.

12. Open the DAPI stained images and binarize with the thresholding routine in the software. To do this, click on **Image > Adjust > Threshold**, and set the appropriate parameters to distinguish the nucleus from the background. Then, click on **Apply > Process > Watershed** to split the aggregate nucleus.

13. After that, use the **Analyze Particles** innate software's function to interpret the binary images. To do this, click on **Analyze** and then on **Analyze Particles** and set the appropriate parameters after this: **size** and **circularity filter** (exclude from analysis objects smaller than 7 µm, bigger than 20 µm, or with a circularity smaller than 0.1 µm).

14. Merge the contour images obtained from DAPI analysis to correspondent immunofluorescent pictures to validate the correct staining.

15. Finally, save the associated data (number of objects, mean area, % of coverage, etc.) for the different biomarkers and quantify the expression at D4 and/or D21 using appropriate quantification software.

2. **Cell culture of commercialized pHGG line, UW479, and patient-derived cell line, BT35**[3]

   1. Culture both cell lines in DMEM/F-12 GlutaMAX supplemented with 10% Fetal Bovine Serum (FBS) in a cell culture flask. Wait for 80% confluence of each cell line as presented in **Figure 1C**.

   2. Maintain these pHGG cells under a controlled environment at 37 °C in normoxic conditions throughout the experiments.

3. Co-culture protocol

1. Adjust the seeding day and concentration for UW479 and BT35 cell lines to reach 80% of confluent cells when co-culture should start, corresponding to 21 days of culture for glutamatergic neurons.

2. Trypsinize UW479 and BT35 cells and seed them on the top of glutamatergic neurons in each dedicated microfluidic device (with a target density of 900 cell/mm^2 for each cell type) before seeding the pHGG cells into the microfluidic device containing matured glutamatergic neurons.

3. Maintain the co-cultures for 2 days under a controlled environment (37 °C, 5% CO_2) with glutamatergic neuron D11 and onward medium detailed in **Table 1**.

4. Count pHGG cells using the microscopic pictures analyzed with an image analysis software to assess their viability. Calculate the percentage of cells.
   NOTE: Use the following formula: 100 - ((number of cells at D23 / number of cells at D21) x 100).

4. Electrophysiological recording

1. Perform the electrophysiological recording with a commercial system and commercially available software.
   NOTE: The experiments were carried out with a MEA that consisted of 30 µm diameter electrodes spaced by 100 µm.
2. Perform a first electrophysiological recording on glutamatergic neurons at D21 before seeding of pHGG cells. Use the differentiated glutamatergic neurons as control and culture them alone in parallel to the co-culture. Do a second recording for both conditions as described in the next step numbered 3.
3. Perform a second electrophysiological recording at D23 (after 2 days of co-culture).

5. Electrophysiological data processing

1. Filter the raw data with a 2^{nd} order Band-pass Butterworth filter (with passband frequencies of 100 Hz and 2500 Hz).
2. For spike detection, compute the root mean square of the signal over the 10 min recording for each electrode and set an amplitude threshold corresponding to eight times this root mean's square value.
3. Apply a PTSD (Precision Timing Spike Detection[25]) algorithm, considering a maximum duration of 2 ms for one action potential.
4. Consider as an active electrode, each electrode detecting at least 5 spikes/min. Continue the assay if at least 10% of the recording electrodes are active.
5. Divide the number of detected spikes by the time-period of recording to calculate the mean firing rate of each active electrode. Calculate an average mean firing rate for each independent experiment. Ultimately, calculate an average by condition (±SEM) and express it as a function on the day of recording.
6. Compute a raster plot for each experiment representing the events detected for each active electrode as a function of time. Then, calculate the temporal array-wide firing rates (or instantaneous firing rates) of all the active electrodes, allowing to monitor synchronicity of the neural network activity.
7. Finally, generate bar graphs using the quantification software and perform comparisons using Kruskal Wallis tests.

Representative Results

Before studying electrical interactions between glutamatergic neurons and glioma cells, hiPS-derived cortical glutamatergic neurons were characterized to validate the feasibility of culturing them in microfluidic devices (**Figure 1A**). Their characterization was assessed using Nestin, Sox2, mGlurR2 (metabotropic Glutamate Receptors 2), and vGLUT1 immunostaining, represented in **Figure 1A(2-7)**. As Nestin is an intermediate filament protein required for survival, renewal and mitogen-stimulated proliferation of neural progenitor cells, it is thus expressed in undifferentiated CNS cells during development. Sox2 is a member of the SRY-like HMG-box gene (SOX) transcription factor family involved in the regulation of embryonic development, and it

is predominantly expressed in immature and undifferentiated cells of the neural epithelium in CNS. mGluR2 is widely distributed throughout the brain, with high expression in the cortex and hippocampus. Usually, it defines the presynaptic cells with their neuronal excitability and synaptic transmission (e.g., the glutamatergic neurons). vGLUT1 is also used as a glutamatergic biomarker. Therefore, **Figure 1** focuses on glutamatergic neurons with Nestin and Sox2 expressions at D4 and D21 to validate their progressive differentiation into the culture conditions (**Figure 1A(2-4)**. Nestin positive cells' percentage decreased from 5.4 ± 0.4% at D4 to 0.69 ± 0.3% at D21 ($p < 0.01$, **Figure 1A5**). Similarly, confirming the differentiated state of glutamatergic neurons, the percentage of Sox2 positive cells decreased from 12.2 ± 2.1% at D4 to 5.5 ± 1.7% at D21 ($p < 0.05$, see **Figure 1A6**). The expression of mGluR2 was detected in 45.4 ± 4.7% of glutamatergic cells at D21 (data not shown), and a larger vGLUT1 immunostaining was observed during glutamatergic differentiation at D21. These results demonstrated that the proportion of neural progenitors remained low and that most cells were well differentiated after a 21-day culture in the microfluidic devices. In **Figure 1B**, a general protocol of the multistep co-cultures and electrophysiological recording describes the UW479 or BT35 cell seeding in the microfluidic devices at D21. Those cell lines (**Figure 1C**) were already described and are comparable to the previous observations made by us[3,19]. In the end, two electrophysiological recordings were obtained: one at D21 before co-culturing and the other at D23 after 48 h of pHGG cell line seeding.

For understanding and following the mobility and viability of BT35, UW479, and glutamatergic neurons during co-cultures, microscopic assessments were regularly performed during the electrophysiological recording period from D21 to D23 and are presented in **Figure 2**. The microscopic images revealed a progressive extension and particular distribution of glutamatergic neurons across microfluidic devices (**Figure 2A**). The glutamatergic cells form some aggregates progressively in a similar way in co-culture and when cultured alone until D23 (control experiment). In **Figure 2B**,**C**, when adding BT35 and UW479, it was observed that the floating cells present immediately after glioma cells' seeding at D21 progressively disappeared until D23 and became adherent pHGG cells into the device. This was particularly notable for the UW479 line.

Moreover, there was no increase in floating cells after all electrophysiological recordings at D23 (data not shown). Nevertheless, the percentages of viable cells in **Figure 2D** were estimated at 83.02% and 85.16% for BT35 and UW479, respectively. Both line viabilities were comparable and underlined the fact that patient-derived cell lines can be used appropriately. The technical preparation of microfluidic devices coupled to MEA and cell manipulations does not alter their adhesion capacities. It does not seem to induce cell death or modify their microscopic aspects. BT35 and UW479 cells seem to map the exact locations of glutamatergic neurons in the device, migrating closely to the excitatory neurons.

Figure 3 describes as an example UW479/glutamatergic neuron co-cultures with their spike detection along recording time in **Figure 3A** and its raster plot at D23 in **Figure 3B**, showing increased electrical activity when adding pHGG cells. **Figure 3C** presents the temporal array-wide firing rate in BT35/glutamatergic neuron co-cultures. The differences between the control experiment (culture of glutamatergic neurons) and co-cultures of glutamatergic neurons with pHGG cells are significant when recording D23 electrical

activity, as shown in **Figure 3D**, which indicates an impact of pHGG on neuron excitability.

Components	Seeding medium	D4 medium	D7 medium	D11 and onward medium
DMEM/F-12 Medium	0.5x	0.25x	0.125x	Ø
Neurobasal Medium	0.5x	0.25x	0.125x	Ø
BrainPhys Medium	Ø	0.5x	0.75x	1x
SM1 Supplement	1x	1x	1x	1x
N2 Supplement-A	1x	1x	1x	1x
Ala-Gln (GlutaMax)	0.5 mM	0.5 mM	0.5 mM	0.5 mM
BDNF	10 ng/mL	10 ng/mL	10 ng/mL	10 ng/mL
GDNF	10 ng/mL	10 ng/mL	10 ng/mL	10 ng/mL
TGF-β1	1 ng/mL	1 ng/mL	1 ng/mL	1 ng/mL
Geltrex	30 µg/mL	Ø	Ø	Ø
Seeding Supplement	1x	Ø	Ø	Ø
Day 4 Supplement	Ø	1x	Ø	Ø

Table 1: Culture media composition for hiPS-derived glutamatergic neurons.

Antibodies	Stock concentrations	Working dilutions
Nestin	0.5 mg/mL	1:500
		(1 µg/mL)
Sox2	1 mg/mL	1:500
		(2 µg/mL)
mGluR2	0.2 mg/mL	1:50
		(4 µg/mL)
vGlut1	0.25 mg/mL	1:50
		(5 µg/mL)
Donkey anti-rabbit IgG H&L (AF 647)	2 mg/mL	1:1000 to 1:2000
		(1 to 2 µg/mL)
Donkey anti-mouse IgG H&L (AF 555)	2 mg/mL	1:1000
		(2 µg/mL)

Table 2: List of immunofluorescent antibodies.

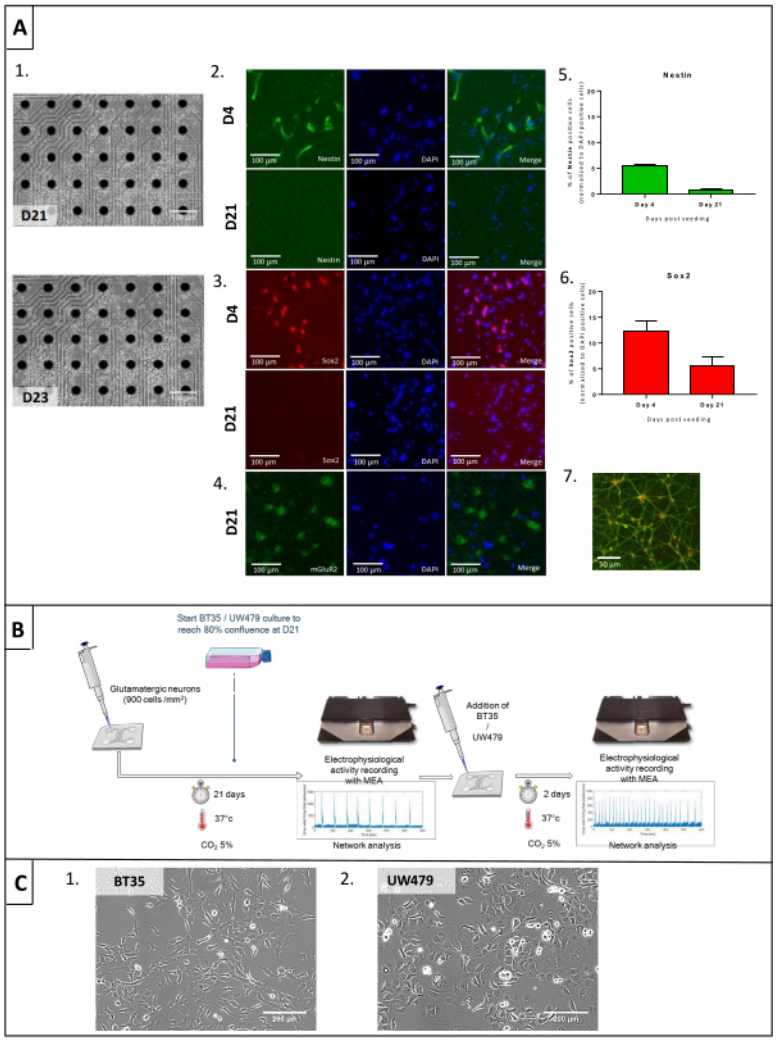

Figure 1: Cell characterization and co-culture protocol of glutamatergic neurons and high-grade pediatric glioma (pHGG) lines. (**A**) Prerequisite microscopic and immunofluorescent characterization of glutamatergic neurons. (**1**) Microscopic pictures at day 21 (D21) and day 23 (D23) of glutamatergic neurons. (**2**) Nestin labeling in green and DAPI in blue at D4 (upper row) and D21 (bottom row). (**3**) Sox2 labeling in green and DAPI in blue at D4 (upper row) and D21 (bottom row). (**4**) mGluR2 labeling in green and DAPI in blue at D21. (**5 and 6**) Statistical comparisons between Nestin and Sox2 labeling at D4 and D21 of culture, demonstrating cell differentiation. (**7**) vGlut1 staining in green and DAPI in orange at D21. (**B**) General protocol for electrophysiological recording to study interactions when co-culturing glutamatergic neurons and glioma cells on devices. (**C**) Prerequisite microscopic aspects of BT35 and UW479 cell lines. Please click here to view a larger version of this figure.

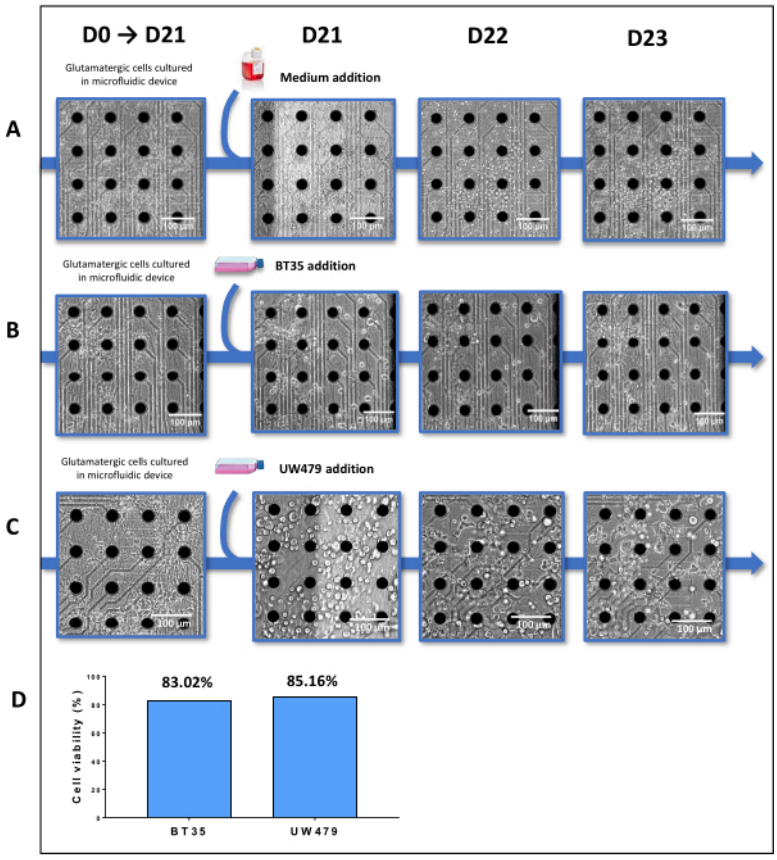

Figure 2: Microscopic images of glutamatergic and glioma cells cultured in microfluidic devices coupled to multielectrode arrays (MEA). Glutamatergic neurons are differentiated and cultured alone in the microfluidic device until day 21 (D21). (**A**) For this experimental control, only the medium was added to glutamatergic cells at D21, while either BT35 (**B**) or UW479 (**C**) cell lines were added in their respective conditions. Images at D22 and D23 were performed before the electrophysiological records for each condition. All the images were obtained using a classical phase-contrast microscope. (**D**) Tumor cell viability for BT35 and UW479 at D23 was estimated using an automated count with image analysis software.

Please click here to view a larger version of this figure.

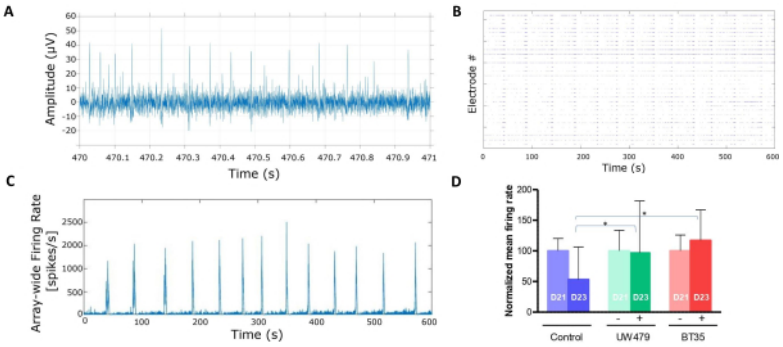

Figure 3: Electrophysiological recording. (**A**) Spike detection along recording time in UW479/glutamatergic neuron co-cultures. (**B**) An example of the computed raster plot at D23 represents the events detected for each active electrode as a function of time in UW479/glutamatergic neuron co-cultures. (**C**) Temporal array-wide firing rate (or instantaneous firing-rate) of all the active electrodes recording electrical activity in BT35/glutamatergic neuron co-cultures, allowing to monitor synchronicity of the neural network activity. (**D**) Bar charts of mean firing rate in the control condition (e.g., the culture of glutamatergic neurons) and when adding tumoral UW479 cell line (in green) and BT35 cell line (in red). Data are shown as mean ± SEM. (* $p < 0.05$). Please click here to view a larger version of this figure.

Supplemental Figure S1: 3D (3-dimensional) representation of SU-8 molds. (**A**) Creation and picturing of SU-8 molds with AutoCAD software. (**B**) Picture of the SU-molds with the two layers of photoresist structures and four holes of 3 mm width. Please click here to download this File.

Discussion

This work describes an accurate functional *in vitro* model to evaluate the interaction between human hiPS-derived cortical glutamatergic neurons and brain tumoral cells in microfluidic devices. One of the crucial steps in the present protocol was the hiPS differentiation in glutamatergic neurons, which was confirmed by the decrease of Nestin and Sox2 immunofluorescent staining and simultaneous appearance of mGluR2 and vGLUT1 staining. Nevertheless, few neural progenitors remained as only half of the glutamatergic cells expressed mGluR2, which means a heterogeneous neuron cell population. Altogether, these results emphasize that particular care must be devoted to glutamatergic cell growth in such devices. Furthermore, the next step studying the electrical behavior of neurons in the presence of pHGG cells was relatively labor-intensive to set up the data processing to optimize the spike detection and interpretation. Nevertheless, as expected and described in other recently published works[4,5,6,9,10], the presence of pHGGs and glutamatergic neurons enhances electrical activity confirming the excitatory feature of those neurons.

The major limitation of this modeling might be the heterogeneous distribution of neurons on the MEA itself that can impact electrophysiological recordings. It would require the maintenance of high-density culture in the microfluidic device. For seeding a secondary cell type onto the device, it is

critical to maintain a rapid proliferation and migration initially for 48 h and obtain as for neurons a homogeneous distribution in the 48 h technique for recording. Another limitation is differentiating the different types of cell populations in such devices visually, but new approaches using fluorescent nanoparticles might help following both cell types[26]. Finally, the performance of this microfluidic approach was only done in two types of phGG lines and should be extended to more patient-derived cell lines bearing different molecular drivers. Complementary assessments might be done to understand this excitatory effect when co-culturing those cells. Nevertheless, it is feasible with pHGG cells bearing an H3.3 K27M driver mutation, such as in the BT35 line[3].

The overall method developed in this work is one of the new approaches to explore the electrical impact. It has shown the capacity of neural network analysis to transduce the interaction between hiPS-derived glutamatergic neurons and pHGG tumoral cell lines in microfluidic culture conditions. This method is helpful for many applications, particularly for functional and mechanistic studies and for analyzing the effects of pharmacological agents that can block pHGG cell migration and interaction with neurons. It emphasizes the use of microfluidic devices, but specifically when experiments might record the electrophysiological activity and can be added to an MEA.

Disclosures

AB, MG, JR, LM, ML, JV, DD are employed by NETRI, FL is Chief Technology Officer at NETRI, and TH is Chief Scientific Officer at NETRI. The other authors have nothing to disclose.

Acknowledgments

This work was supported by grants from Satt Conectus program, Fondation de l'Université de Strasbourg, «J'ai demandé la lune», «Une roulade pour Charline», «LifePink», «Franck, Rayon de Soleil» and «Semeurs d'Etoile» associations. We thank the children and families affected by HGGs for their contributions to this research and their support.

References

1. Mackay, A. et al. Integrated molecular meta-analysis of 1,000 pediatric high-grade and diffuse intrinsic pontine glioma. *Cancer Cell.* **32** (4), 520-537 (2017).
2. Ostrom, Q. T. et al. Alex's lemonade stand foundation infant and childhood primary brain and central nervous system tumors diagnosed in the United States in 2007-2011. *Neuro-Oncology.* **16** (Suppl 10), x1-X36 (2015).
3. Blandin, A. F. et al. Hypoxic environment and paired hierarchical 3D and 2D models of pediatric *H3.3*-mutated gliomas recreate the patient tumor complexity. *Cancers (Basel).* **11** (12), 1875 (2019).
4. Monje, M. Synaptic communication in brain cancer. *Cancer Research.* **80** (14), 2979-2982 (2020).
5. Mount, C. W., Yalçın, B., Cunliffe-Koehler, K., Sundaresh, S., Monje, M. Monosynaptic tracing maps brain-wide afferent oligodendrocyte precursor cell connectivity. *eLife.* **18** (8), e49291 (2019).
6. Venkatesh, H. S. et al. Electrical and synaptic integration of glioma into neural circuits. *Nature.* **573** (7775), 539-545 (2019).
7. Blanco-Suárez, E., Caldwell, A. L., Allen, N. J. Role of astrocyte-synapse interactions in CNS disorders. *Journal of Physiology.* **595** (6), 1903-1916 (2017).

8. Neftel, C. et al. An integrative model of cellular states, plasticity, and genetics for glioblastoma. *Cell.* **178** (4), 835-849 (2019).
9. Krishna, S. et al. Glioblastoma remodeling of neural circuits in the human brain decreases survival. *BioRxiv* .(2021).
10. Venkataramani, V. et al. Glutamatergic synaptic input to glioma cells drives brain tumour progression. *Nature.* **573** (7775), 532-538 (2019).
11. Wang, X. et al. Reciprocal signaling between glioblastoma stem cells and differentiated tumor cells promotes malignant progression. *Cell Stem Cell.* **22** (4), 514-528 (2018).
12. Venkatesh, H. S. et al. Targeting neuronal activity-regulated neuroligin-3 dependency in high-grade glioma. *Nature.* **549** (7673), 533-537 (2017).
13. Venkatesh, H. S. et al. Neuronal activity promotes glioma growth through Neuroligin-3 secretion. *Cell.* **161** (4), 803-816 (2015).
14. Buckingham, S. C. et al. Glutamate release by primary brain tumors induces epileptic activity. *Nature Medicine.* **17** (10), 1269-1274 (2011).
15. Campbell, S. L., Buckingham, S. C., Sontheimer, H. Human glioma cells induce hyperexcitability in cortical networks.*Epilepsia.* **53** (8), 1360-1370 (2012).
16. Maisonneuve, B. G. C., Vieira, J., Larramendy, F., Honegger, T. Microchannel patterning strategies for in vitro structural connectivity modulation of neural networks. *BioRxiv.* (2021).
17. Pastore, V. P., Godjoski, A., Martinoia, S., Massobrio, P. SpiCoDyn: A toolbox for the analysis of neuronal network dynamics and connectivity from multi-site spike signal recordings. *Neuroinformatics.* **16** (1), 15-30 (2018).
18. Honegger, T., Thielen, M. I., Feizi, S., Sanjana, N. E., Voldman, J. Microfluidic neurite guidance to study structure-function relationships in topologically-complex population-based neural networks.*Scientific Reports.* **6**, 28384 (2016).
19. Nguyen, A. et al. Characterization of the transcriptional and metabolic responses of pediatric high grade gliomas to mTOR-HIF-1α axis inhibition. *Oncotarget.* **8** (42), 71597-71617 (2017).
20. Taylor, A. M., Dieterich, D. C., Ito, H. T., Kim, S. A., Schuman, E. M. Microfluidic local perfusion chambers for the visualization and manipulation of synapses. *Neuron.* **66** (1), 57-68 (2010).
21. Cerea, A. et al. Selective intracellular delivery and intracellular recordings combined in MEA biosensors. *Lab on a Chip.* **18** (22), 3492-3500 (2018).
22. Bruno, G. et al. Microfluidic multielectrode arrays for spatially localized drug delivery and electrical recordings of primary neuronal cultures. *Frontiers in Bioengineering and Biotechnology.* **8**, 626 (2020).
23. Park, J. W., Vahidi, B., Taylor, A. M., Rhee, S. W., Jeon, N. L. Microfluidic culture platform for neuroscience research. *Nature Protocols.* **1** (4), 2128-2136 (2006).
24. Maisonneuve, B. G. C. et al. Deposition chamber technology as building blocks for a standardized brain on chip framework. *BioRxiv.* (2021).
25. Maccione, A. et al. A novel algorithm for precise identification of spikes in extracellularly recorded neuronal signals. *Journal of Neuroscience Methods.* **177** (1), 241-249 (2009).

26. Andreiuk, B. et al. Fluorescent polymer nanoparticles for cell barcoding in vitro and in vivo. *Small.* **13** (38) (2017).